J Solid State Electrochem (2012) 16:2261–2265
DOI 10.1007/s10008-011-1635-x

ORIGINAL PAPER

p-Type behaviour of electrodeposited ZnO:Cu films

Bernabé Marí · Mustapha Sahal · Miguel A. Mollar · Fatima M. Cerqueira · Anura P. Samantilleke

Received: 7 October 2011 / Revised: 13 December 2011 / Accepted: 27 December 2011 / Published online: 8 February 2012

Abstract Cu-doped ZnO (ZnO:Cu) thin films and ZnO/ZnO:Cu homojunction devices were electrodeposited on conductive glass substrates in a non-aqueous electrolyte containing Cu and Zn salts. The Cu content of the films is proportional to the Cu/Zn precursor ratio in the deposition electrolyte. ZnO:Cu was found to be of a hexagonal wurtzite structure with (002) preferred orientation. A transition from n-type to p-type was observed for ZnO:Cu films with a Cu/Zn ratio higher than 2% as inferred from the change in the direction of the photocurrent. The rectifying characteristics shown by homojunction devices further confirm the p-type conductivity of ZnO:Cu layers.

Keywords ZnO:Cu · *p*-type · Electrodeposition · Photocurrent · ZnO homojunction

Introduction

ZnO is a wide band gap semiconductor material that has recently drawn significant attention as a strong candidate for numerous electronic applications [1]. However, p-type doping of ZnO is extremely difficult due to the presence of native defects and donors. The primary reason hindering the deposition of high-quality p-type ZnO is the formation of native donor defects (NDD), such as O vacancies and Zn interstitials, when ZnO is synthesized under O-poor conditions [2]. Therefore, to avoid the formation of NDD, a solution would be to grow ZnO films under O-rich conditions and substitute Zn by elements belonging to group IA (Li, Na and K) or group IB (Cu, Ag and Au) [3]. However, although substitutional group IA elements make shallow acceptors, it has been found that they tend to occupy the interstitial sites in ZnO where they behave as donors and impede the p-type [4]. Thus, group IB elements have been proposed as the best possible candidates for *p*-type ZnO doping [5]. Theoretical studies predict that Cu-doped ZnO can exhibit p-type behaviour [6], and both p- and n-type behaviours have been reported for Cu-doped ZnO using vacuum deposition methods [7–9].

In recent years, electrodeposition (ED) has emerged as an attractive, low-cost method for growing thin film semiconductors [10]. For example, the authors have already reported on several ternary ZnMO films (M=Cd, Co, Mn, Fe) [11–14] synthesized by ED. In this paper, we report on the electrochemical synthesis and structural, optical and photoelectrochemical characterization of Cu-doped ZnO films exhibiting p-type behaviour.

Experimental

The ED was carried out in a three-electrode electrochemical cell, consisting of a transparent conductive oxide (TCO—indium tin oxide, ITO, or fluorine-doped tin oxide, FTO)-coated glass with a sheet resistance of 9 Ω/square as the working electrode, a Pt counter electrode and a Ag/AgCl (+0.222 V vs normal hydrogen electrode) reference electrode. The potential is reported in the text with respect to

B. Marí (✉) · M. Sahal · M. A. Mollar
Department de Física Aplicada-IDF,
Universitat Politècnica de València,
Camí de Vera s/n,
46022 València, Spain
e-mail: bmari@fis.upv.es

F. M. Cerqueira · A. P. Samantilleke
Centro de Fisica, Universidade do Minho,
Braga 4710-057, Portugal

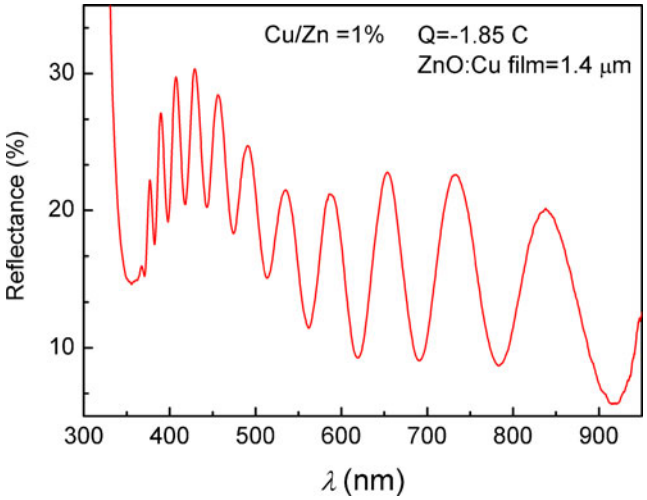

Fig. 1 Reflectance spectrum of the ZnO:Cu thin film obtained from a starting solution containing a ratio Cu/Zn=0.01

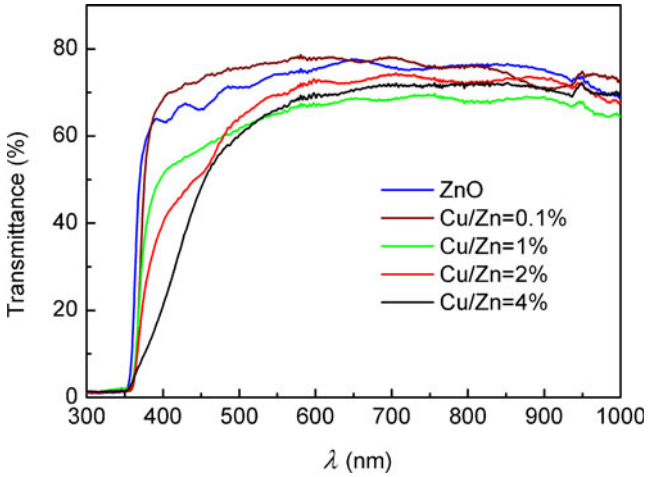

Fig. 2 Transmittance spectra of ZnO:Cu electrodeposited thin films with different copper concentrations

the Ag/AgCl electrode. TCO substrates and were pre-cleaned with double-distilled water and subsequently rinsed with acetone, ethanol and dried. The electrolytes were prepared by dissolving zinc perchlorate hexahydrate [$Zn(ClO_4)_2{\cdot}6H_2O$] and copper perchlorate hexahydrate [$Cu(ClO_4)_2{\cdot}6H_2O$] in dimethylsulfoxide (DMSO). The concentration of zinc perchlorate hexahydrate was 25 mM, and the concentration of copper perchlorate hexahydrate was below 1 mM.

In contrast to ZnO electrodeposited in aqueous media, where the morphologies (rods, columns, wire, etc.) are often discontinuous [15], ZnO:Cu electrodeposited in DMSO offers continuous smooth depositions [16]. The smoothness of such deposits causes the surfaces to behave in perfect plano-parallel layers.

Potassium perchlorate [$KClO_4$] 0.1 M was used as the supporting electrolyte while the solution was saturated with O_2 by purging. The Cu/Zn ratio of the electrolyte was varied between 0% and 4%. All ACS Reagents were supplied by Sigma-Aldrich and used without prior purification. The deposition was carried out through the application of a constant potential −0.9 V vs Ag/AgCl electrode on the working electrode at 80 °C. The size of TCO substrates was 2 cm^2, and the films were deposited over a surface of 1 cm^2. The deposited charge was between 1 and 2 C, so the specific charge per unit area ranged from 1 and 2 C/cm^2. The deposited films were subsequently rinsed with distilled water and acetone. The chemical, structural and optical properties of the as-grown ZnCuO thin films were characterized.

Table 1 (1) Copper/zinc ratio in the starting electrolyte, (2) final Cu/Zn fraction in electrodeposited thin films measured by EDX, (3) full width at half maximum (FWHM) of the peak (002), (4) crystallite size

(1) Starting Cu/Zn	(2) Cu/Zn in the film	(3) FWHM (°)	(4) Crystallites size (Å)
0	0	0.2090	416
0.01	0.024	0.1909	455
0.02	0.038	0.2056	423
0.03	0.076	0.2221	391
0.04	0.086	0.3600	241

Results and discussion

A typical specular reflectance spectrum of a thin film ZnO:Cu is shown in Fig. 1. The thickness calculated from the interference fringes of thin film was found to be 1.4"m, after subtracting the TCO contribution, which is very close to the estimated thickness using the Faraday equation [17].

Columns 1 and 2 in Table 1 report the Cu/Zn ratio existing in the solid film as a function of the Cu^{2+}/Zn^{2+} ion ratio added in the starting electrolyte. The Cu/Zn ratio inside thin films, as determined by energy dispersive spectroscopy, is twice the Cu^{2+}/Zn^{2+} ion ratio in the initial electrolyte due to the diffusion-controlled deposition of Cu.

The reduction of Zn takes place according to the following reaction:

$Zn^{2+}+2e \rightarrow Zn$ (−0.76 V vs normal hydrogen electrode, NHE).

However, the reduction of Cu takes place at a more positive potential with respect to Zn, $Cu^{2+}+2e \rightarrow Cu$ (+0.34 V vs NHE).

At the ZnO deposition potential (−0.9 V vs Ag/AgCl electrode), Cu is co-deposited with Zn.

Figure 2 shows the transmittance spectra of ZnO:Cu films for different Cu concentrations. The effect of Cu

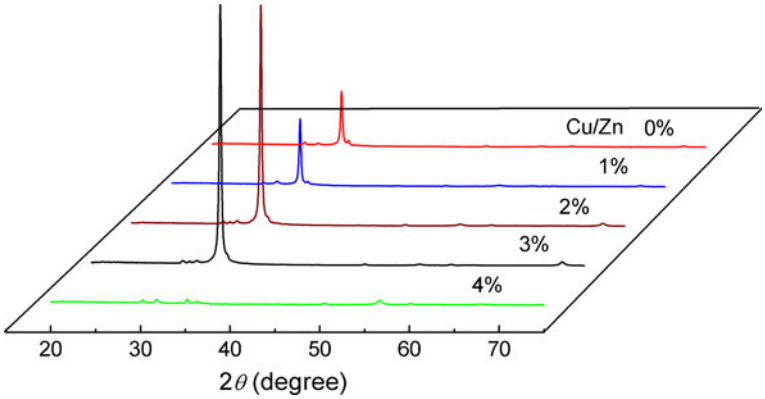

Fig. 3 XRD spectra of ZnO:Cu films for different Cu concentrations

doping red shifts the absorption edge, suggesting a narrowing of the optical bandgap of the doped films. The low formation energy enables the incorporation of a high concentration of Cu defects into ZnO, forming a defect band and narrowing the bandgap of ZnO [5]. Furthermore, the sharp absorption edge, characteristic of the wurtzite ZnO, is apparent for all samples, except for the highest doped sample, in which the absorption edge extends between 360 and 460 nm.

The x-ray diffraction (XRD) spectra of ZnO:Cu films for different concentrations of Cu (Fig. 3) show a wurtzite structure, typical of ZnO, in (002) preferred orientation. The intensity of the (002) peak increases with doping up to 3% Cu/Zn. Further increases in impurity doping cause structural deterioration. This observation is understandable as the preferential orientation of thin films is affected by the surface free energy of each crystal plane as the films usually grow to minimise the surface free energy. As the texture improves with doping up to 4% Cu/Zn, the average crystallite size evidently increases as well (Table 1, columns 3 and 4), which has previously been observed in electrodeposited doped ZnO [10, 11]. As the dopant concentration increases to Cu/Zn=4%, the wurtzite crystal structure is only residual and the texture changes from (002) to (100) and (110) directions. The average crystallite size decreases below the size of pure ZnO crystallites.

As shown in Fig. 4, two Raman modes, the E_2 (high) (440 cm^{-1}) and the A_1 longitudinal optical (A_1 (LO)) (566 cm^{-1}), were observed for undoped ZnO. The A_1 (LO) mode is commonly attributed to the presence of defects in the ZnO lattice such as O vacancies. The weak signal at 580 cm^{-1} superimposes the two modes A_1 (LO) and E_1 (LO). The intensity of both the E_2 (high) mode and A_1 (E_1) increases with doping up to 1% Cu. The peak at 325 cm^{-1}, though clearly noticeable for 1% doped sample, is present in all the samples and is assigned to the second-order Raman scattering arising from zone-boundary phonons E_2 (M) of ZnO. The intensities of E_2 (high) and A_1 (LO) modes were significantly reduced when further increasing Cu, suggesting structural degradation of ZnO due to Cu interaction. However, a relaxation of the ZnO lattice was evidenced with Cu doping when the E_2 peak position shifted to the bulk ZnO position (437 cm^{-1}) from the stressed state of undoped ZnO as evidenced by the blue shift of the E_2 peak position (440 cm^{-1}). With E_2 (M) disappearing with 4% Cu doping,

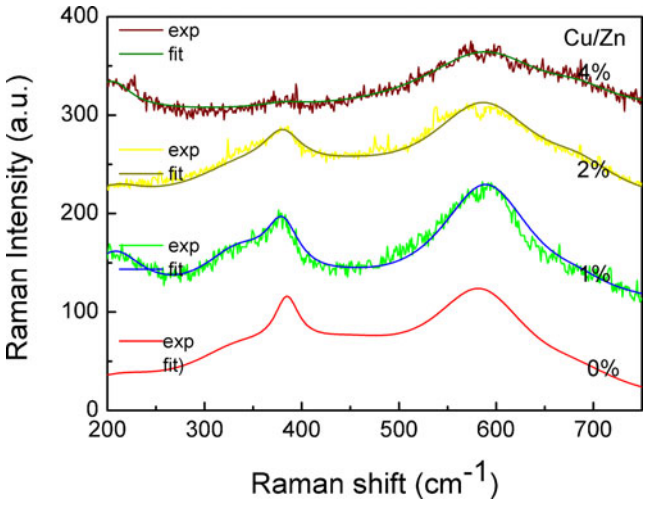

Fig. 4 Micro-Raman spectra for ZnO:Cu electrodeposited films

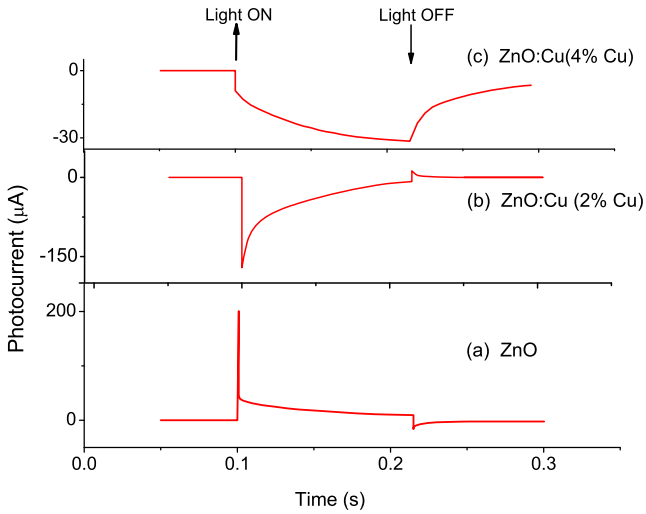

Fig. 5 Time-resolved photocurrent transients in ZnO:Cu films with different Cu contents: **a** undoped ZnO, **b** Cu/Zn=2%, **c** Cu/Zn=4%

a peak at 276 cm^{-1} appeared, which corresponds to a wurtzite–ZnO silent mode allowed by breakdown of the translational crystal symmetry induced by defects and impurities [18]. The presence of Cu interstitials is the likely cause of both the diminishing intensity of E_2 (high) mode and this silent mode. The presence of the E_2 high mode in all the spectra indicates that the doped films still maintain a hexagonal structure.

Time-resolved photocurrent (TRP) transients under white light illumination of ZnO:Cu films in contact with electrolytes are shown in Fig. 5. Upon illumination, undoped or doped with Cu/Zn=1% films in contact with 1 M Na_2SO_3 electrolyte, a strong hole scavenger, show a more positive photocurrent than the dark current, while the films with higher Cu content (Cu/Zn~2%) show negative photocurrent when in contact with the Eu^{3+}/Eu^{2+} electrolyte, suggesting p-type conductivity [19, 20]. The lower photocurrent observed for the films with higher Cu content (Cu/Zn=4%) was also reflected in significantly different electrode kinetics. No overshoots were detected in TRP measurements for the (Cu/Zn=4%) films, indicating recombination reactions of the charge carriers.

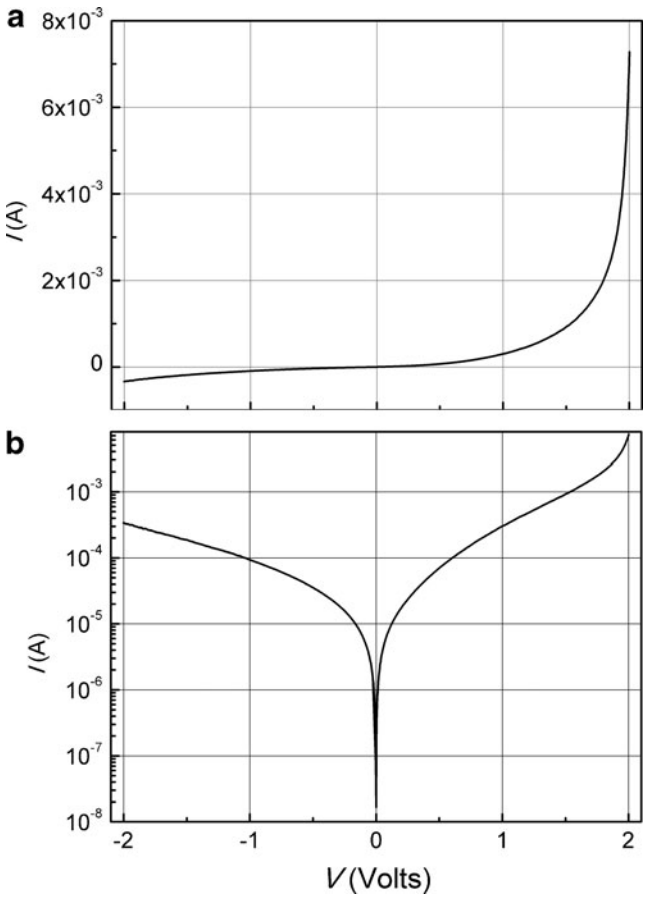

Fig. 6 *I*-V curves (**a** linear and **b** log I vs V) of a ZnO/ZnO:Cu homojunction device

A homojunction was fabricated by depositing a ZnO:Cu layer on top of a ZnO/ITO, and the device was completed by vacuum evaporating an Au layer. The I-V characteristics of these devices are shown in Fig. 6, supporting the suggestion that the electrodeposited ZnO:Cu layer behaves as a p-type semiconductor. Although the leakage is high, the rectification behaviour indicates the device to be a p-n junction. The high leakage is attributed to the degeneracy of the p-ZnO (ZnO:Cu) induced by high Cu doping in these devices. The I!V curve also shows a small leakage current under reverse bias, possibly due to the defect states introduced by Cu doping, which act as recombination centres. The rectification factors for the ITO/ZnO/ZnO:Cu/Au device 22 for ±2 V, which can be improved by reducing porosity of the ZnO layers and further controlling the defect density.

Conclusion

Cu-doped ZnO thin films and ZnO:Cu/ZnO homojunction devices were electrochemically synthesized using DMSO electrolyte. A transition from n-type to p-type behaviour was observed in ZnO:Cu films when the Cu/Zn ratio is about 2%. With 4% Cu doping, breakdown of the translational crystal symmetry induced by defects and impurities associated with Cu dopant was observed. The rectification factor of p-n junction devices at 2 V reached a maximum value of 22. Further work includes fine tuning of optimum Cu doping, essential in reducing the leakage current observed in the devices due to defect states introduced by Cu doping.

Acknowledgements This work was supported by the Spanish Government through MEC grant MAT2009-14625-C03-03 and the Portuguese Foundation for Science and Technology (FCT), CIENCIA 2007. Financial support by the European Commission through NanoCIS project (PIRSESGA-2010-269279) is gratefully acknowledged.

References

1. Klingshirn C (2007) Phys Status Solidi B 244:3027–3073
2. Lyons JL, Janotti A, Van de Walle CG (2009) Appl Phys Lett 95:252105–252107
3. Zunger A (2008) Appl Phys Lett 83:1830–1832
4. Park CH, Zhang SB, Wie S (2002) Phys Rev B 66:073202–073204
5. Yan Y, Al-Jassim MM, Wie S (2006) Appl Phys Lett 89:181912–181914
6. Park MS, Min BI (2003) Phys Rev B 68:224436–224441
7. Shukla G (2009) Appl Phys A 97:115–118
8. Buchholz DB, Chang RPH, Song JH, Ketterson JB (2005) Appl Phys Lett 87:82504–82506
9. Rahmani MB, Keshmiri SH, Shafiei M, Latham K, Wlodarski W, du Plessis J, Kalantar-Zadeh K (2009) Sensor Letters 7:621–628
10. Lincot D (2005) Thin Solid Films 487:40–48
11. Tortosa M, Mollar M, Marí B (2007) J Crystal Growth 304:97–102

12. Tortosa M, Mollar M, Marí B, Lloret F (2008) J Appl Phys 104:033910–033914
13. Mollar M, Tortosa M, Casasús R, Marí B (2009) Microelectronics J 40:276–279
14. Marí B, Elmanouni A, Damonte L, Mollar M (2010) Phys Status Solidi A 207:1623–1626
15. Cembrero J, Busquets-Mataix D (2008) Thin Solid Films 517:2859–2864
16. Marí B, Cembrero J, Mollar M, Tortosa M (2008) Phys Status Solidi C 5:555–558
17. Fisicaro P, Adriaens A, Ferrara E, Prenesti E (2007) Anal Chim Acta 597:75–81
18. Manjón FJ, Marí B, Serrano BJ, Romero AH (2005) J Appl Phys 97:053516–053519
19. Rajeshawar K (2001) Fundamentals of semiconductor electrochemistry and photoelectrochemistry. In: Licht S (ed) Encyclopedia of electrochemistry. Wiley-VCH, Weinheim, pp 38–39
20. Zoski CG (2007) Handbook of electrochemistry. Elsevier, Amsterdam, pp 336–358